

On Cyclostationary Analysis of WiFi Signals for Direction Estimation

Changlai Du Huacheng Zeng Wenjing Lou Y. Thomas Hou
Virginia Tech, Blacksburg, VA, USA

Abstract—Cyclostationary analysis is a powerful tool to study the Signal-Selective Direction Estimation (SSDE) problem as different types of wireless signals have different cyclostationary patterns. Generally speaking, each type of wireless signal has unique cyclic frequencies with the frequency-selective property, which distinguishes itself from other types of signals. The cyclostationary property of a signal may be induced by its modulation method, its carrier frequency, and/or its frame structure. In this paper, we study the cyclostationary property of IEEE 802.11 (WiFi) signals induced by their underlying OFDM frame structure, which includes pilots, cyclic prefix (CP), and preambles. We first analyze the pilot-induced, CP-induced, and preamble-induced cyclostationary properties of WiFi signals, respectively. We then derive their spectral correlation function (SCF) and investigate their applicability to solving the SSDE problem. Simulation results show that the pilot-induced cyclostationary property of WiFi signals is a promising feature that can be used to solve the SSDE problem.

I. INTRODUCTION

Wireless communication has become ubiquitous all over the world. In indoor environments, IEEE 802.11 (WiFi) is the predominant wireless communication solution. However, due to the “open air” property of wireless media and the crowded unlicensed ISM band, WiFi communication may be easily interfered with by itself or other ISM systems (e.g., Bluetooth). When WiFi communication is interrupted by interference, quick and accurate detection and localization of the interfering source is of great importance to resolve the problem, especially in business scenarios like enterprises and hospitals. If the interfering source can be localized it is easy to restore WiFi communication (e.g., by turning off the interfering source). Signal-Selective Direction Estimation (SSDE) is a popular method for interfering source localization. The basic idea of SSDE is to compute the coordinates of the interfering source based on the Angle of Arrival (AoA) of the line-of-sight signal from the interfering source at a set of anchoring WiFi nodes [1], [2], [7]. A prerequisite, which is also a major challenge, of the SSDE problem is that at an anchoring WiFi node, one should distinguish the signal of the targeted interference source from the signals of other (interfering or desired) signal sources.

Cyclostationary based direction estimation algorithms (see [7]) have been proposed to address this challenge, by exploiting the signal selection properties of cyclic frequencies. A signal can be modeled as cyclostationary if its cyclic autocorrelation function (CAF) is nonzero for some nonzero cyclic frequencies. The Spectral correlation function (SCF) is the Fourier transform of a CAF, which can be estimated

efficiently from discrete samples of the signals. A cyclic frequency is a frequency at which the CAF is not zero, which can be determined by examining the peaks on the signal CAF or SCF surfaces. Once a cyclic frequency of the target signal is identified, the Cyclic MUSIC algorithm [11] can be used to estimate the signal AoA. The Cyclic MUSIC algorithm takes a cyclic frequency of the target signal as an input, and then performs the MUSIC algorithm in [1] to estimate only the desired signal directions of arrival. Therefore, estimation of signal cyclic frequencies is the first step to exploit the Cyclic MUSIC algorithm for direction estimation. A thorough analysis and evaluation of WiFi cyclostationary properties needs to be performed to estimate signal cyclic frequencies.

OFDM is widely used as the modulation technique for major communication applications such as WiFi (IEEE 802.11a/g/n) to improve spectrum efficiency. For the purpose of signaling, channel estimation, and synchronization, OFDM frame structure introduces some features including pilots, cyclic prefix (CP), and preambles. These features generate peaks on the SCF surface at specific cyclic frequencies, which can be utilized to distinguish WiFi signals from other signals.

In this paper, we analyze WiFi cyclostationarity induced by these OFDM features. We first present the signal models of these features and then derive their spectral correlation functions. After that, we investigate the applicability of the induced cyclic frequencies to the SSDE problem. Simulation was conducted and the results are in agreement with our theoretical analysis. To the best of our knowledge, we are the first to analyze the cyclostationary properties of OFDM-based WiFi signals thoroughly for this purpose. The analysis results (e.g., OFDM feature induced cyclostationarity) are also useful for other applications, such as signal detection and identification in the Cognitive Radio (CR) networks.

The rest of the paper is organized as follows. Related work is presented in section II. Section III offers essential background of the cyclostationary analysis. Section IV presents the cyclostationary analysis induced by OFDM features of WiFi. In section V we evaluate the influence of these features on the direction estimation of WiFi signals. Section VI concludes the paper.

II. RELATED WORK

Cyclostationary analysis is widely studied for the purpose of signal detection and identification. In [4], the authors proposed an OFDM system identification scheme for CR networks based on pilot-induced cyclostationarity. In [3], an

embedded cyclostationary signature method for OFDM-based waveform identification was proposed. They generated a cyclostationary signature using OFDM subcarrier set mapping, thus a spectral correlation was created in each OFDM symbol by simultaneously transmitting data symbols on more than one subcarrier. In [5], [6], [16], the authors discussed pilot-induced and preamble-induced cyclostationarity as well as their applications for signal detection in CR networks.

Cyclostationary property based interfering radio localization was proposed in [8], [9]. In these papers, the authors exploited cyclostationary analysis to extract feature vectors to detect signal types, the occupied spectrum, and the AoAs of arriving signals at the detecting radio. However, the authors did not provide the details of how cyclic frequencies (in these papers named pattern frequencies) were generated. They only gave a conclusion that the pattern frequencies of WiFi is any one between $[f_c - \frac{BW}{2}, f_c + \frac{BW}{2}]$ in [8]. Our work is inspired by these two papers, with a focus on the how cyclostationary properties are induced by WiFi OFDM structures.

III. CYCLOSTATIONARITY BACKGROUND

In this section, we introduce the concept of signal *cyclostationary* properties and the Cyclic MUSIC algorithm.

A. Cyclostationary

A signal can be modeled as cyclostationary if its cyclic autocorrelation function (CAF) is nonzero for a nonzero cyclic frequency. The *Cyclic Autocorrelation Function* (CAF) is defined by

$$\mathbf{R}_x^\alpha(\tau) \triangleq \langle x(t + \tau/2)x^*(t - \tau/2)e^{-j2\pi\alpha t} \rangle, \quad (1)$$

where the $\langle \cdot \rangle$ is the time averaging operation defined by

$$\langle \cdot \rangle \triangleq \lim_{T \rightarrow \infty} \frac{1}{T} \int_{-T/2}^{T/2} (\cdot) dt.$$

If for some cyclic frequency α and delay τ , $\mathbf{R}_x^\alpha(\tau) \neq 0$, then this signal x is a cyclostationary signal. When $\alpha = 0$, $\mathbf{R}_x^\alpha(\tau)$ reduces to a conventional autocorrelation function.

Equation (1) can be further interpreted as

$$\mathbf{R}_{uv}(\tau) = \langle u(t + \tau/2)v^*(t - \tau/2) \rangle, \quad (2)$$

where $u(t) = x(t)e^{-j\pi\alpha t}$ and $v(t) = x(t)e^{j\pi\alpha t}$.

We can see from Equation (2) that a signal exhibiting the cyclostationary property correlates with a frequency-shifted version of itself, which means that the signal exhibits the spectral coherence property.

The Fourier transform of CAF is *spectral correlation function* (SCF), which is defined by

$$\begin{aligned} \mathbf{S}_x^\alpha(f) &= \int_{-\infty}^{\infty} \mathbf{R}_x^\alpha(\tau) e^{-j2\pi f\tau} d\tau \\ &= \lim_{B \rightarrow 0} \frac{1}{B} \langle [h_B^f(t) \otimes u(t)][h_B^f(t) \otimes v(t)]^* \rangle, \end{aligned} \quad (3)$$

where \otimes denotes convolution, $u(t)$ and $v(t)$ are given in Equation (2), and $h_B^f(t)$ is the impulse response of a one-sided bandpass filter with center frequency f (see [7] for details).

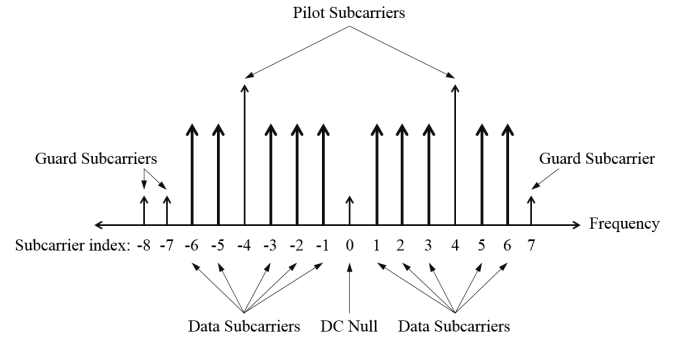


Fig. 1: OFDM Subcarriers. Ten data subcarriers and two pilot subcarriers are included. Three guard subcarriers and a DC Null are also depicted. All the subcarriers are indexed.

In the discrete domain, the continuous signal $x(t)$ is sampled as a series $x[n]$ and the values of SCF must be estimated from the samples. The algorithm we choose here is Fast Fourier Transform (FFT) accumulation (FAM) [10].

B. Cyclic MUSIC algorithm

The MUSIC [1] algorithm and its improved versions [2] estimate the signal directions by performing an eigendecomposition on the covariance matrix of the data collected from an antenna array. The directions of incoming signals are estimated at the intersection of the steering vector for the antenna array and the signal subspace.

Cyclic MUSIC [11] algorithms automatically classify signals based on their known spectral correlation properties and estimate only the desired signals' directions of arrival. Cyclic MUSIC algorithms perform singular value decomposition on the signals' *cyclic autocorrelation matrix* defined in Equation (1). Improved Cyclic MUSIC algorithms [13], [14] perform singular value decomposition (SVD) on composition of the cyclic autocorrelation matrix.

The incoming signals can be written as

$$x(t) = \sum_{i=1}^I s_i(t) + n(t),$$

where $s_i(t)$ is the i th incoming signal, $n(t)$ is the noise, and I is the number of incoming signals. Then we have

$$\mathbf{S}_x^\alpha(f) = \sum_{i=1}^I \mathbf{S}_{s_i}^\alpha(f) + \mathbf{S}_n^\alpha(f). \quad (4)$$

For signal i which has a particular cyclic frequency α_i , the SCF in Equation (4) can be simplified to

$$\mathbf{S}_x^{\alpha_i}(f) = \mathbf{S}_{s_i}^{\alpha_i}(f). \quad (5)$$

This equation follows from the fact that at cyclic frequency α_i , all other signals and noise are uncorrelated with s_i . This is the *signal selection property* of cyclic frequencies, which we exploit to solve the SSDE problem.

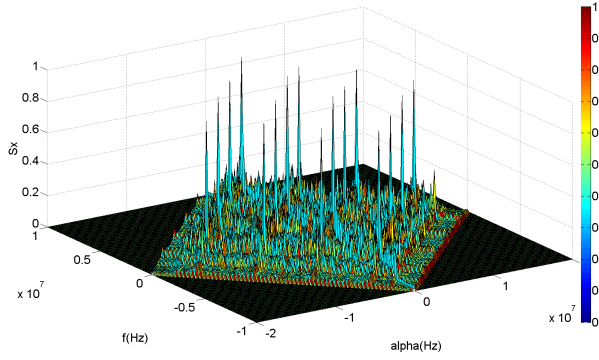


Fig. 2: Pilot-induced SCF peaks for 64-point FFT OFDM. The indices of pilot subcarriers are set to $\{-21, -7, 7, 21\}$.

IV. WiFi CYCLOSTATIONARY ANALYSIS

OFDM is a modulation scheme that uses multiple carriers to transmit data. For the purpose of signaling, channel estimation, and synchronization, OFDM frame structure introduces some features including pilots, CP, and preambles. In this section, we analyze the cyclostationary properties induced by these features.

A. Pilot-Induced Cyclostationarity

Pilots are a key component in the structure of OFDM signals, making it possible to perform channel estimation and frequency compensation. Fig. 1 illustrates the subcarrier layout of a 16 subcarrier OFDM structure [6]. Ten data subcarriers and two pilot subcarriers are adopted in this structure. Three guard subcarriers and a DC Null are also depicted. All the subcarriers are indexed by the offset to DC Null. Data values are random complex numbers while the pilots are fixed complex numbers. As the pilots are fixed and of higher power, they exhibit some peaks on their SCF surface over data and noise, where a cyclostationary pattern is formed.

The discrete-time baseband transmitted OFDM signal with pilots (but without CP¹) can be modeled as

$$x(m) = \sqrt{\frac{E_s}{N}} [x_d(m) + x_t(m)], \quad (6)$$

where

$$x_d(m) = \sum_k \sum_{\substack{n=0 \\ n \notin \mathcal{I}}}^{N-1} a_k(n) e^{j2\pi \frac{n}{N}(m-kN)} \cdot q(m-kN)$$

and

$$x_t(m) = \sum_k \sum_{n \in \mathcal{I}}^{N-1} b_k(n) e^{j2\pi \frac{n}{N}(m-kN)} \cdot q(m-kN).$$

E_s is the signal power and $a_k(n)$ is the transmitted data at the n th subcarrier of the k th OFDM symbol. \mathcal{I} denotes the set of pilot subcarrier indices and $b_k(n)$ is the pilot symbols. $q(m)$

¹The cyclostationary feature of CP in OFDM signals will be analyzed later.

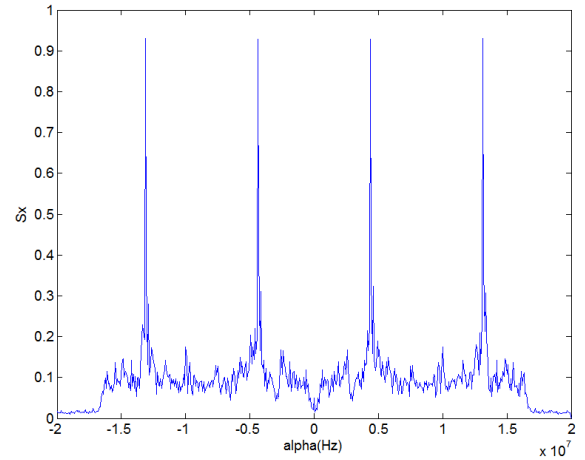


Fig. 3: Cyclic frequencies when $f = 0$. The cyclic frequencies are $\alpha = \pm 4.375$ MHz, ± 13.125 MHz.



Fig. 4: IEEE 802.11 b/g OFDM frame structure [15]. The OFDM structure contains features that generate cyclostationary properties: pilots, CP, and preambles.

is the pulse shaping filter. For WiFi, the pilot's index subset \mathcal{I} stays the same with all OFDM symbols and is determined by the implementation.

From Equation (3), it is easily derived that the SCF surface peaks when the frequency-shifted versions of the OFDM subcarrier layouts align at a pilot subcarrier. Take Fig. 1 as an example, when $\alpha = 0$, SCF peaks at $f = \pm 4B$, where B is subcarrier frequency spacing. For simplicity, we omit B afterward, and use the index numbers to indicate the frequencies. Further, when $\alpha = \pm 8$, SCF peaks at $f = 0$.

In general, suppose that OFDM signals have $2K$ pilots evenly and symmetrically distributed and the index distance between two adjacent pilots is $2p$, then SCF peaks at

$$\begin{aligned} \alpha &= \pm 4kp, & f &= \pm p, \pm 3p, \dots, \pm(2K-1-2k)p, \\ \alpha &= \pm(4k+2)p, & f &= 0, \pm 2p, \dots, \pm(2K-2-2k)p, \end{aligned} \quad (7)$$

where $0 < k < K$.

Fig. 2 and 3 illustrate the simulation results of the SCF of OFDM with no CP. The number of subcarriers is $N = 64$, with 48 data subcarriers, 4 pilot subcarriers and 12 null subcarriers. The sampling frequency is 20 MHz (with subcarrier spacing of 325 kHz). The indices of subcarriers are set to $\{-21, -7, 7, 21\}$. We can see from Fig. 3 that when $f = 0$, the peaks of the SCF surface appears at the cyclic frequencies $\alpha = \pm 4.375$ MHz, ± 13.125 MHz. We note that in order to

illustrate the SCF peaks, the power of pilot subcarriers is given a 6 dB gain.

B. CP-Induced Cyclostationarity

In OFDM modulation, the data and pilot on the frequency subcarriers are converted to time-domain signals via IFFT operations. A CP is then inserted into the OFDM symbol by copying a portion of the higher index IFFT output samples and appending it to the front of the OFDM symbol. The purpose of the CP is to combat Inter-Symbol Interference (ISI) between neighboring OFDM symbols caused by transmission in a multipath channel.

Fig. 4 depicts IEEE 802.11 a/g OFDM frame structure, which has 64-point IFFT operations and a CP of 16 points. For a 20 MHz sampling frequency, a standard OFDM symbol with CP is $4\mu s$ in time duration.

The discrete-time baseband OFDM signal with CP can be modeled as

$$x(m) = \sqrt{\frac{E_s}{N}} \sum_k \sum_{n=0}^{N-1} a_k(n) e^{j2\pi \frac{n}{N} (m-D-k(N+D))} \cdot q(m-k(N+D)), \quad (8)$$

where D is the number of points of CP and $a_k(n)$ is an independent and identically distributed (i.i.d) message symbol sequence. Notice that in this model we only consider CP-induced cyclostationarity, as pilot-induced cyclostationarity has been studied in the previous subsection.

The spectral correlation can be derived as:

$$S_x^\alpha(f) = \begin{cases} \frac{E_s}{N} \sum_{n=0}^{N-1} Q(f - \frac{n}{N} + \alpha/2) \cdot Q^*(f - \frac{n}{N} - \alpha/2) & \alpha = \frac{d}{N+D} \\ 0 & \alpha \neq \frac{d}{N+D} \end{cases} \quad (9)$$

where $Q(f) = \frac{\sin(\frac{\pi f}{f_s})}{\pi f}$ is the Fourier transform of the square shaping pulse $q(m)$.

From Equation (9) we can see that CP-induced peaks at the bi-frequency SCD surface appear at $\frac{d}{N+D}$, where $d \in \mathbb{Z}$. Fig. 5 illustrates the simulation results of the SCF for OFDM with $N = 64$, $D = N/4$, and sampling frequency $F = 20$ MHz. We note that to illustrate CP-induced cyclostationarity more clearly, the cyclic frequency resolution of the FAM algorithm is set to $F/256$ in the simulation, so that the SCF peaks only at $\pm \frac{5l}{4}$ MHz, with $l \in \{1..13\}$.

C. Preamble-Induced Cyclostationarity

A WiFi physical protocol layer data unit (PPDU) begins with a preamble. As depicted in Fig. 4, the preamble consists of two parts: the short and long preamble training sequences. The preamble in an OFDM signal is designed to provide the means to estimate the channel, estimate frequency offset, and identify the beginning of the OFDM signal through a preamble correlation process. Different OFDM implementations have distinct preamble patterns, which enables the receiver to detect

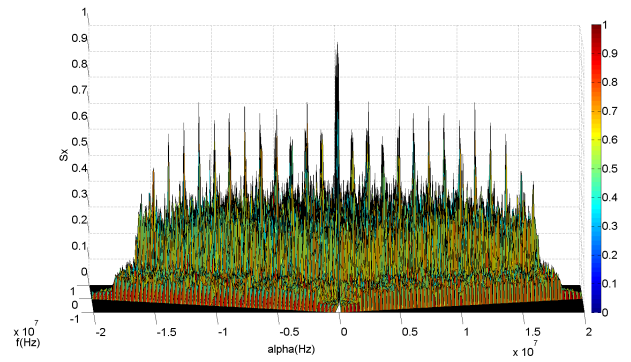


Fig. 5: CP-induced Cyclostationarity. SCF surface peaks at the cyclic frequencies $\pm \frac{5l}{4}$ MHz, with $l \in \{1..13\}$

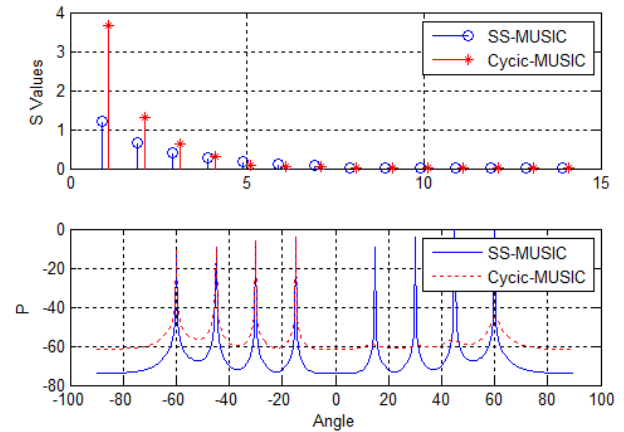


Fig. 6: Cyclic MUSIC and Spatial Smoothing MUSIC. Cyclic MUSIC decreases the ratio of the largest undesired singular value and the smallest desired singular value.

the presence of a compliant signal. Although it seems to be a promising method of signal identification by cyclostationary analysis, the random WiFi package transmission pattern makes it impossible.

It is worth pointing out that the strategy of inserting specific subcarrier patterns into preambles to induce cyclostationarity does not work for our purpose. This is because in the SSDE problem it is assumed that we have no control of the signal structure of the interfering sources.

V. PERFORMANCE EVALUATION

In this section, we evaluate how these (pilot-induced and CP-induced) cyclic frequencies perform when using them in Cyclic MUSIC algorithms to estimate the signal direction of arrival. We evaluate their performance by conducting simulation in Matlab, the simulation parameters are listed in Table I.

We assume that there are two signal sources: one WiFi and one Bluetooth. The channel from each signal source to the anchoring node for detection consists of 4 multipath components. An antenna array with 16 sensors (i.e., 16 antenna elements) in a Uniform Linear Array (ULA) are used to

TABLE I: Simulation Parameters

FFT size	64
Sampling frequency	20 MHz
Subcarrier spacing	0.325 MHz
# of data subcarriers	48
# of pilot subcarriers	4
Pilot subcarrier index	-21, -7, 7, 21
# of OFDM frames	10
WiFi signal AoAs	-60, -45, -30, -15
Bluetooth Signal AoAs	15, 30, 45, 60
# of array sensors	16
Sensor space	0.5 wavelength
Pilot gain	2.5 dB

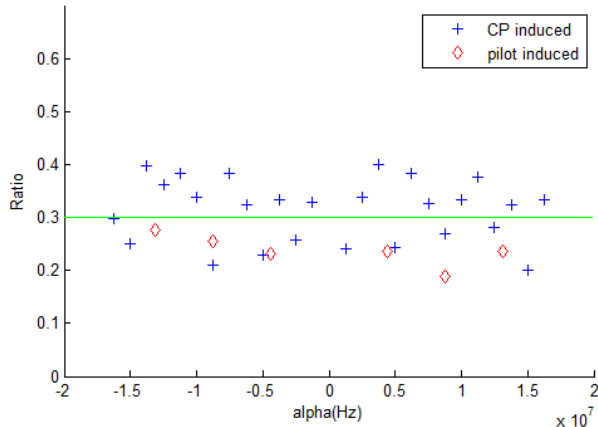


Fig. 7: Ratios of singular values. The ratio values calculated by pilot-induced cyclic frequencies are smaller than those by CP-induced cyclic frequencies.

collect signals from the signal sources. Two AoA estimation algorithms are employed for the purpose of comparison: Spatial smoothing MUSIC algorithm (SS-MUSIC) in [12] and Cyclic MUSIC algorithm with spatial smoothing in [11]. Although SS-MUSIC is not able to distinguish different types of signals, SS-MUSIC efficiently eliminates the correlation between multipath components of the same signal source.

MUSIC-based AoA estimation algorithms differentiate signals and noises according to their corresponding singular values (or eigenvalues). Intuitively, Cyclic MUSIC algorithm will decrease the singular values of undesired signals at proper cyclic frequencies, which make them easier to differentiate. Simulation results in Fig. 6 illustrate this effect, where singular values after the 5th point are decreased.

Based on this consideration, we employ the ratio of the largest undesired singular value and the smallest desired singular value as a metric to evaluate the performance of different cyclic frequencies in the SSDE problem.

Fig. 7 depicts the simulation results. The ratio values are the average of 50 runs. From the figure we can see that the ratio values calculated by pilot-induced cyclic frequencies are smaller than those by CP-induced cyclic frequencies, which indicates that at pilot-induced cyclic frequencies, it is easier to distinguish desired signals from undesired signals. Suppose that the threshold value is set to 0.3, as depicted

in Fig. 7. We can see that pilot-induced cyclic frequencies can differentiate noise successfully while some of the CP-induced cyclic frequencies cannot. We thus conclude that pilot-induced cyclic frequencies are better than CP-induced cyclic frequencies to solve the SSDE problem.

VI. CONCLUSIONS

In this paper, we analyzed the cyclostationary property of IEEE 802.11 (WiFi) signals induced by the features of underlying OFDM frame structure, including pilots, CP, and preambles. We studied the influence of these features on the signal's spectral correlation function. We also evaluated the applicability of the induced cyclic frequencies to solve the SSDE problem. Simulation results confirmed that pilot-induced cyclic frequencies are a better approach for the SSDE problem when compared to CP-induced cyclic frequencies. Following the current results, future work will be undertaken to estimate the localization of interference radios by exploiting the estimated cyclic frequencies and signal directions.

REFERENCES

- [1] R. O. Schmidt, "Multiple emitter location and signal parameter estimation," *IEEE Transactions on Antennas and Propagation*, vol. 34, no. 3, pp. 276–280, Mar 1986.
- [2] R. Roy and T. Kailath, "ESPRIT-estimation of signal parameters via rotational invariance techniques," *IEEE Transactions on Acoustics, Speech and Signal Processing*, vol. 37, no. 7, pp. 984–995, Jul 1989.
- [3] P. D. Sutton, K. E. Nolan, and L. E. Doyle, "Cyclostationary signatures in practical cognitive radio applications," *IEEE Journal on Selected Areas in Communications*, vol. 26, no. 1, pp. 13–24, Jan. 2008.
- [4] F.-X. Socheleau, P. Ciblat, and S. Houcke, "OFDM system identification for cognitive radio based on pilot-induced cyclostationarity," in *Proc. of IEEE WCNC*, Budapest, Hungary, April 2009.
- [5] M. E. Castro, "Cyclostationary detection for ofdm in cognitive radio systems," Master's thesis, Faculty of The Graduate College at the University of Nebraska.
- [6] S. R. Schnur, "Identification and Classification of OFDM based signals using preamble correlation cyclostationary feature extraction," Naval Postgraduate School, Monterey CA, Sep. 2009.
- [7] W. A. Gardner, "Exploitation of spectral redundancy in cyclostationary signals," *IEEE Signal Processing Magazine*, vol. 8, no. 2, pp. 14–36, April 1991.
- [8] S. Hong and S. Katti, "DOF: A local wireless information plane," in *Proc. ACM SIGCOMM*, Toronto, Canada, Aug. 2011.
- [9] K. Joshi, S. Hong, and S. Katti, "PinPoint: localizing interfering radios," in *Proc. of USENIX NSDI*, Berkeley, CA, April 2013.
- [10] R. S. Roberts, W. A. Brown, and H. H. Loomis, "Computationally efficient algorithms for cyclic spectral analysis," *IEEE Signal Processing Magazine*, vol. 8, no. 2, pp. 38–49, April 1991.
- [11] S. V. Schell, R. A. Calabretta, W. A. Gardner, and B. G. Agee, "Cyclic MUSIC algorithms for signal-selective direction estimation," in *Proc. of International Conference on Acoustics, Speech, and Signal Processing*, vol. 4, pp. 2278–2281, May 1989.
- [12] J. Xiong and K. Jamieson, "ArrayTrack: a fine-grained indoor location system," in *USENIX NSDI*, Berkeley, CA, April 2013.
- [13] P. Charge, Y. Wang, and S. Joseph, "An extended cyclic MUSIC algorithm," *IEEE Transactions on Signal Processing*, vol. 51, no. 7, pp. 1695–1701, July 2003.
- [14] W.-J. Zeng, X.-L. Li, X.-D. Zhang, and X. Jiang, "An improved signal-selective direction finding algorithm using second-order cyclic statistics," in *Proc. of IEEE ICASSP*, pp. 2141–2144, Taipei, Taiwan, April 2009.
- [15] *Wireless LAN medium access control (MAC) and physical layer (PHY) specifications*, IEEE 802.11.
- [16] K. Maeda, A. Benjebbour, T. Asai, T. Furuno, and T. Ohya, "Cyclostationarity-inducing transmission methods for recognition among OFDM-Based systems," *EURASIP Journal on Wireless Communications and Networking*, Jan. 2008.